Inter-Data Center Network Dimensioning under Time-of-Use Pricing

Burak Kantarci, *Senior Member, IEEE* and Hussein T. Mouftah, *Life Fellow, IEEE*

Abstract—In the cloud era, data centers consume tremendous power due to their huge computing and storage requirements. Furthermore, allocation and release of resources by numerous cloud customers leads to significant energy consumption at the data centers, which in turn, increases the Operational expenditures (Opex) of the operators. In this article, we combine energy efficiency and Time of Use (ToU)-awareness, and propose a novel virtualization scheme, namely ToU-aware Provisioning (ToUP) for an inter-data center network over an IP over WDM backbone. In ToUP, in addition to the traffic between two backbone nodes, upstream user demands destined to data centers and downstream data center demands originating from many data centers; inter-data center traffic is also considered for workload sharing between the data centers. Initially, we present an MILP formulation to model the optimal behavior of ToUP. Since the inter-data center network needs to be reconfigured in polynomial time, we propose a simulated annealing (SA)-based heuristic. We verify the heuristic by using the MILP solution as the benchmark. We evaluate ToUP under various scenarios, and numerical results confirm that significant Opex savings can be achieved while demands can be provisioned with low energy consumption in the data centers and network equipments.

Index Terms—Cloud computing, data centers, energy efficiency, inter-data center network, IP over WDM, Time-Of-Use, virtual topology

1 Introduction

Cloud computing has emerged on the cutting edge of the Information and Communication Technologies (ICTs) by combining the advantages of various computing paradigms in order to run business more efficiently [1], [2]. In order to meet increasing demand in clouds, corporate data centers (DCs) need to be transformed and consolidated into cloud data centers which are constructed on large terrains with enhanced capacity and energy efficiency. On the other hand, challenges such as security, energy efficiency and automated service provisioning in cloud computing need to be addressed. As the amount of data intensive applications increase in the Cloud, utilization of large numbers of physical servers (i.e., nodes) increase dramatically not only for computing reasons but for also replication purposes [3]. Therefore, among these challenges, energy efficiency in the Cloud seems to be a significant issue due to the enormous increase in Greenhouse Gas (GHG) emissions of data centers [4] and the operational expenditures (Opex) of data center operators [5], namely the electricity bills.

In [6], the authors point out the essentiality of the balance between storage, process and transport energies. Therefore energy efficiency in cloud computing has several aspects such as energy-aware workload and virtual machine placement on the physical servers [7], [8], thermal monitoring of the data centers to manage intra-data center workload scheduling [4], [9], and energy efficient Cloud service provisioning over the backbone network [10], [11], [12] via intelligent deployment of anycast/manycast-based communication protocols. Furthermore, network and data center resource utilization is drastically increased due to parallel job submissions to various destination data centers and downloading high volumes of real time and/or non-real time data which consequently increase the power consumption and the electricity bills of the network and data center operators [13], [14].

Here, taking advantage of dynamic pricing tariffs in smart grids can help reduce Opex of the operators while ensuring fairness among network nodes in terms of power consumption. Hereafter we use the terms Opex and electricity bills interchangeably. The most popular approaches among existing time varying tariffs are Time-of-Use (ToU) pricing [15], Real Time Pricing (RTP) [16] and Critical Peak Pricing (CPP) [17]. ToU denotes determining differentiated electricity prices during different timeslots of the day in advance of power usage where electricity prices are determined by the utilities in real time in order to manage their profit and reduce peak-to-average load ratio on the power grid. Customers can also reduce their electric bills by following ToU rates. Although several benefits of RTP have been discussed in academia and industry, the authors in [18] report ToU pricing to be more viable today due to the following main reasons. First, customers that have been charged flat rates may be reluctant to join RTP-based programs where electricity prices vary more frequently. Second, customers may not easily adapt to the elasticity of RTP tariffs. Following this specification, in [19] we have analyzed the impact of ToU-aware demand provisioning in the

- *B. Kantarci is with the Department of Electrical and Computer Engineering, at Clarkson University, Potsdam, NY 13699. E-mail: bkantarc@clarkson.edu.*
- *H.T. Mouftah is with the School of Electrical Engineering and Computer Science, University of Ottawa, Ottawa, ON K1N6N5, Canada. E-mail: mouftah@site.uottawa.ca.*

Manuscript received 9 Dec. 2013; revised 27 Oct. 2014; accepted 1 Nov. 2014. Date of publication 14 Nov. 2014; date of current version 7 Dec. 2016. Recommended for acceptance by M. Hasan.
For information on obtaining reprints of this article, please send e-mail to: reprints@ieee.org, and reference the Digital Object Identifier below.
Digital Object Identifier no. 10.1109/TCC.2014.2371037

Cloud backbone as the inter-data center (IDC) network switches between several virtual topologies periodically based on look-ahead demand forecast. The study in [19] reports that taking advantage of multiple time zones in the inter-data center network enables reduction in the electricity bills of the network and data center operators while introducing longer provisioning delays for the user demands that are submitted to the data centers. In [20], ToU-awareness has been extended to include inter-data center traffic. To this end, the authors have briefly presented a simulated annealing (SA)-based heuristic which determines the inter-data center load sharing map and integrates ToU-awareness into previously proposed Delay and Power Minimized Provisioning (DePoMiP) [10].

This paper is an extension of the study in [19], [20]. It is assumed that short term forecast is possible for the Cloud demand profiles [21], [22], [23], [24], and each backbone node is assumed to be associated with a data center. Based on the look-ahead demand profile, the Cloud backbone is reconfigured to switch to a new virtual topology to accommodate the forecasted demands with low Opex, low power consumption, and low path delay. To this end, a Mixed Integer Linear Programming (MILP) model is presented and explained in detail where data centers are assumed to share their workload over an IP over Wavelength Division Multiplexing (WDM) medium. In order to avoid excessive network traffic and service quality degradation for the users, each data center is assumed to be allowed to migrate at most a certain amount (i.e., 1-κ_{MIN}) of its total workload to one or more data centers.

Routing the user demand towards one destination out of a set of eligible destinations is referred as anycast whereas routing towards a subset of the eligible destinations is called manycast. In a Cloud network, a downstream demand consists of multiple streams originating from several data centers, and it is routed towards a core node based on the unicast paradigm whereas an upstream user demand is routed based on the anycast/manycast paradigm. Thus, unlike the conventional communication modes such as unicast and multicast, in cloud computing, user requests are towards one or more data centers in the Cloud, and the destination(s) is (are) not determined at the time of job submission. It is assumed that four types of demands co-exist in the Cloud network as follows:

i) *Downstream data center demands.* A downstream DC demand originates from multiple data centers in the form of multiple unicast streams, and it is destined to a backbone node.
ii) *Upstream DC demands.* An upstream DC demand originates from a core node, and it is routed towards several data centers based on the manycast paradigm. In a network with the set of nodes, V, manycast denotes the communication mode where a source node transmits data to a subset of a set of eligible destinations (i.e., $\{s, \widehat{D_s} \subseteq D_s \subseteq D \subseteq V\}$, see Table 1 for the notation).
iii) *Inter-data center demands.* An IDC demand originates from a data center, and it is routed towards several data centers based on the manycast paradigm.
iv) *Non-DC demands.* A non-DC demand denotes unicast traffic between two core nodes. Non-DC demands can also be called the regular Internet demands.

In order to facilitate reconfiguring the backbone topology in polynomial time, we present the ToU-aware provisioning (ToUP) heuristic in detail which aims at minimum electricity costs for the data center and network operators, as well as lowest possible path delay for each demand type. We initially test the sub-optimality of ToUP heuristic under small scale scenarios. Therefore, we compare its performance to the results obtained via solution of the Mixed Integer Linear Programming model. Here, by sub-optimality, we denote the proximity of the heuristic results to the results obtained from the solution of the MILP formulation. Performance metrics in this comparison are electricity cost, power consumption, network resource consumption and path delay. Once the ToUP heuristic is shown to be in reasonable proximity to the solution of the MILP-based model, we present the Simulated Annealing-based heuristic in detail, which aims at obtaining a DC workload sharing map (Map) where Map_{ij} denotes the percentage of workload migration from DC-i to DC-j. Through simulations, we show that ToUP reduces the electricity costs for the data center operator as well as the network operator when compared to the legacy delay and energy-minimized provisioning schemes in [10]. Furthermore, when inter-DC workload sharing is enabled in ToUP, further savings in the electricity bills are possible. We further study the impact of κ_{MIN} (see Table 1) on the Opex and delay performance of the inter-data center network, and show that limiting the allowable workload migration among data centers ($\kappa_{MIN} < 1$) can also reduce path delays for inter-data center workload migration while cutting the electric bills of data center and network operators.

The paper is organized as follows. Section 2 briefly introduces the related work and motivation of this study. In Section 3, we present the MILP formulation which serves as a benchmark for ToUP. Then, we present the SA-based heuristic to obtain the load sharing map of the data centers. In Section 4, we present and discuss the numerical results. We conclude the paper and give future directions in Section 5.

2 Related Work and Motivation

To the best of our knowledge, ToU-aware cuts in the electricity bills for unicast demand provisioning has initially been considered in [25] for an optical WDM network. We have initially studied ToU-based electricity bill cuts in an inter-data center network in [19] where an MILP model has been implemented with the objective of minimum electricity cost for the data center and the network operators. Thus, the MILP formulation aims at traversing the routes with lowest ToU electricity prices and for the manycast demands, reaching the data centers at the regions where lowest ToU prices are being experienced. We have reported that adopting ToU-aware provisioning can cut the electricity bills of data center operators to some extent although these savings can increase the electricity expenses of the network operator, as well as the path delay for the upstream DC demands. In [26], the authors have proposed an MILP formulation to re-distribute the

TABLE 1
The Notation Used in the Formulation

Notation	Explanation
V	Set of nodes/data centers.
N_i^v (N_i^p)	Set of neighboring nodes of node-i in the virtual (physical) topology.
D_s	Set of eligible destinations for the demands initiated at node-s.
$\widehat{D_s}$	Set of selected destinations, i.e, $\widehat{D_s} \subseteq D_s$.
$O_n(T)$	Opex of the network operator for the period T.
$O_{dc}(T)$	Opex of the data center operator for T.
$T_{start}(T_{end})$	Start (end) of the period T.
P_r	Power consumption of an IP router port.
$C_{ij}(C'_{ij})$	Number of active (available) virtual links between node-i and node-j.
W_{mn}^{ij}	Number of lightpaths traversing the physical link-mn in the virtual link-ij.
C	Capacity of a wavelength channel.
Lf_{mn}	Fiber link length between node-m and node-n.
$\varphi_i(T)$	ToU electricity price at the location of node-i during period T.
P_t	Power consumption of a transponder.
W_{ij}	Number of available channels in the virtual link.
W	Number of active channels in a fiber link.
S_{ij}	Number of Erbium Doped Fiber Amplifiers (EDFAs) in the physical link-ij.
f_{ij}	Number of fibers in the physical link-ij.
P_e	Power consumption of an EDFA.
Φ_s^i	Additional cooling and processing power consumption introduced to data center at node-i due to placing the demands of the users at node-s.
$\hbar(\cdot)$	Function that returns the additional cooling and processing power consumption introduced to a data center due to workload migration from other data centers.
ℓ_i	Initial load of data center-i.
ℓ_{MAX}	Maximum load of a data center.
κ_s^i	Ratio of the workload migrated from data center-s to data center-i to the initial load of the data center-s during current virtualization period.
κ_{MIN}	Minimum ratio of the workload that must be hosted in a data center.
$\nabla_s^d\$$	Z times the migrated workload ratio κ_s^d, where Z is a large integer and a multiple of ten.
$\aleph_{ij}^{sd}$	Gets the value of ∇_s^d if the workload migrated from data center-s to data center-d utilizes the virtual link-ij; otherwise it is zero.
Υ_{up}^{sd}	Size of possible demand from node-s to data center-d.
Υ_{down}^{ds}	Size of the demand from data center-s to node-d.
Υ_{IDC}^{sd}	Possible workload migration size from data center-s to data center-d.
Λ_{sd}	Non-DC demand size from node-s to node-d.
$\gamma_{ij_{up}}^{sd}\left(\gamma_{ij_{down}}^{ds}\right)$	Binary variable is one if the upstream (downstream) demand from node-s (data center-s) to data center-d (node-d) utilizes the virtual link-ij.
$\gamma_{ij_{idc}}^{sd}$	Binary variable is one if IDC demand from data center-s to data center-d utilizes virtual link-ij.
λ_{ij}^{sd}	Binary variable is one if the regular demand from node-s to node-d utilizes the virtual link-ij.
$D_{max}^s\left(D_{min}^s\right)$	Maximum (minimum) number of destinations for the upstream traffic from node-s.
DC_{MAX}	Maximum number of possible destinations for an IDC demand.
Ω_s^{UP}	Upstream traffic (job submission) to data centers from node-s.
Ω_{ds}^{DOWN}	Downstream demand from DC-d to node-s.

workloads in a group of data centers so that electricity bills of the operator can be cut. In [27], the authors have proposed an electricity bill capping algorithm. The algorithm initially distributes the requests among data centers by considering location-based electricity pricing, and in its second step, it aims at maximum request throughput of the customers within the budget limit obtained in the first step.

We have also studied energy efficient delivery of the Cloud services over the Internet backbone by focusing on energy efficient routing in IP networks and/or energy efficient anycast/manycast routing and wavelength assignment (RWA) in WDM networks [28].

In [29], the authors have studied the problem of energy efficient lightpath selection based on anycast routing in optical clouds. Recently, in [30], a distributed framework has been proposed for energy efficient management of the lightpaths in the computational grids. Utilization of renewable energy sources is essential to reduce the GHG emissions; hence in [31], [32], the authors have studied the problem of optimal location of data centers considering the availability of the renewable sources. Furthermore, based on the fact that the IP routers are the dominant power consumers in core networks, the authors propose an anycast-based provisioning framework in order to minimize the utilization of non-renewable energy while bypassing the IP routers and enforcing the traffic to be transported in the optical layer as much as possible. In [33], the authors have proposed renewable sources-aware routing algorithms to provision Cloud services in data centers based on the anycast paradigm in an IP over WDM network. In [10], we have studied MILP-based and heuristic design of the inter-data center network with the objective of minimum power consumption in the data centers and the network equipments. Although these studies have considered IP over WDM backbone for provisioning of Cloud services, they have not studied the effect of varying electricity costs with respect to time and location. Furthermore, the impact of varying electricity costs on the Opex of the network and data center operators is still an open issue.

In [34], the authors propose partitioning the data centers that are distributed among different regions to ensure lowering the carbon emissions for the Cloud, electricity expenses and networking costs. The authors in [35] study determining the location of data centers as a crucial problem to ensure green cloud computing networks. As an alternative to VM-based cloud service provisioning, the authors in [36] have proposed mapping virtual data centers (VDC) onto the physical data centers among diverse regions in order to reduce carbon footprint while at the same time increasing the revenue of the cloud provider.

This paper extends the previous work on ToU-aware demand provisioning in the inter-data center network [19], considers the presence of regular, upstream DC and downstream DC demands as well as IDC demands in order to minimize the Opex of the data center and network operators while minimizing the energy consumption in the Cloud backbone throughout the day. Furthermore, we aim at investigating the impacts of the ToU-aware inter-data center network design on the power consumption and electricity costs.

This study aims at filling the following gaps in the literature:

i) Energy efficient design of an IP over WDM network to accommodate cloud computing and regular Internet demands have been studied in the literature without consideration of interaction with the smart grid network in order to enable ToU pricing [10], [31].

ii) ToU pricing has been considered only for all-optical networks [25] however ToU-aware design in an IP/WDM inter-data center network has not been considered yet.

iii) ToU pricing-based provisioning has not been considered with the existence of regular Internet demands and downstream/upstream (i.e., manycast) cloud computing demands.

iv) Although ToU-based workload management in data centers has been studied, the effect of data center workloads on the transport network under ToU-aware demand provisioning has not been considered before.

3 ToU-Aware Provisioning in the Cloud

We consider an integrated architecture consisting of the inter-data center network and the Smart Grid Communication Network (SGCN) [37]. The inter-data center network consists of an IP over WDM transport network and the data centers associated with the backbone nodes. In certain timeslots of the day, based on the changes in the demand profile, the inter-data center network is virtualized in order to achieve the design goals, namely energy efficiency and minimum electricity costs for the network and data center operators. A virtual link denotes a transparent optical lightpath consisting of several physical links. Furthermore, by combining optical bypass technology and topology virtualization, the traffic can be kept in the optical domain without going through the intermediate IP routers. The virtualized inter-data center network communicates with the SGCN in order to retrieve ToU prices at different locations, and this information is used in the next virtualization period. Operation of the virtual inter-data center network is adopted from [38].

The clients are served through the virtualized inter-data center which offers transparent optical lightpaths and light-trees for the demands in accordance with their demand specifications. The service coordinator (SC) is responsible for identifying the type of arriving demand and determining its resource requirement. Resource reservation at the data centers is performed by the resource coordinator (RC). Since resource reservation denotes reservation of both computing and communication resources, the RC works in coordination with the network resource manager (NRM) and the computing resource managers (CRM), each of which is associated with a data center.

ToU-aware Provisioning adopts the Opex minimization approach in [19]. ToUP is based on the following assumptions:

- All demands (i.e., downstream DC, upstream DC, IDC and other regular Internet demands) are routed over an IP over WDM network consisting of N nodes employing optical bypass technology [39].
- Each backbone node is associated with a data center, i.e., data center-i is associated with node-i. Overhead of the access routers is not considered.
- Demand profiles of all types are forecasted periodically. Based on the forecasted demand volumes arriving at each backbone node, a new virtual backbone topology is designed and mapped onto the physical topology.
- Each data center is assumed to have an initial workload, and the power consumption overhead of any job submission and/or migrated workload to a data center is known in advance.

The main objective of ToUP is to minimize the Opex of both data center and network operators. To this end, it aims at accommodating the demands at those locations where ToU rates are lower. Since IP router ports are the most power hungry components in the backbone network [39], their utilization must be minimized by keeping the traffic in the optical domain as long as possible.

In this section, we present an MILP formulation for ToUP and a simulated annealing-based heuristic solution for the model. Before we proceed with the MILP formulation, we present the notation used in the formulation in Table 1. It is worth noting that all power consumption metrics are in watts, and all demand sizes are in Gbps. In the formulation, s always denotes the source node of a demand, and D denotes the set of all destinations for the demands that are initiated at node-s unless otherwise specified.

3.1 An MILP Model for ToUP

The MILP model for ToUP aims at minimizing the Opex of the network and data center operators as formulated by the objective function in Eq. (1)

$$minimize \sum_{i \in V} O_n^i(T) + O_{dc}^i(T). \tag{1}$$

Opex constraints. Opex of the network operator at node-i is the product of the energy consumption of the network equipment during the period T ($T_{end} - T_{start}$) and the electricity price during T at the location of node-i as shown in Eq. (2). The energy consumption of the network equipment at node-i is formulated as the sum of the energy consumed by the IP router ports, transponders and the active Erbium Doped Fiber Amplifiers (EDFAs) deployed on the unidirectional links from node-i to its neighbors. Equation (3) formulates Opex of the data center operator for the data center associated with node-i. According to the equation, Opex at the associated data center of node-i is the product of the prospective energy consumption of the data center, the electricity price during the corresponding interval, and the duration of the interval, T. The prospective energy consumption of data center-i is denoted by the sum of the additional cooling and processing power consumption introduced to it by the users at node-s, additional cooling and processing power introduced to it by the users of the other data centers in the network and power consumption savings due to workload migration from the data center-i to the other data centers in the network.

Here, it is worth noting that the additional cooling and processing power consumption introduced to data center-i by the workload migrated from the other data centers is considered to be a function of the workload migrated to data center-i. In the equation, $\hbar$, denoting the workload migrated from data center-s to data center-i, is a function of the initial workload on data center-s (ℓ_s) and the ratio of its workload migrated to data center-i (κ_s^i)

$$\begin{aligned} O_n^i(T) = &\sum_{j \in N_i^v} P_r \cdot C_{ij} \cdot \varphi_i(T) \cdot (T_{end} - T_{start}) \\ &+ \sum_{j \in N_i^p} (P_t \cdot W_{ij} + S_{ij} \cdot P_e \cdot f_{ij}) \cdot \varphi_i(T) \cdot (T_{end} - T_{start}) \end{aligned} \tag{2}$$

$$\begin{aligned} O_{dc}^i(T) = &\left[\sum_{s \neq i, s, i \in V} \left(\Phi_s^i + \hbar(\ell_s \cdot \kappa_s^i) - \hbar(\ell_i \cdot \kappa_i^s) \right) \right] \cdot \varphi_i(T) \\ &\cdot (T_{end} - T_{start}), \forall i \in V. \end{aligned} \tag{3}$$

IDC constraints. As defined in Table 1, ∇_s^d is Z times the migrated workload ratio, κ_s^d, from data center-s to data center-d. Equation (4) formulates this definition. If the IDC traffic from data center-s to data center-d utilizes the virtual link-ij, then the demand on the corresponding link is expected to be a function of the migrated workload ratio from data center-s to data center-d, i.e., ∇_s^d / Z. The utilized capacity on the corresponding link depends on whether the selected route towards data center-d traverses that link, i.e., $\nabla_s^d \times \gamma_{ij_{idc}}^{sd}$. However, this multiplication leads to non-linearity in the MILP formulation. Therefore, the multiplication is linearized by Eqs. (5)-(7). Details of the linearization method can be found in [40]

$$\nabla_s^d - Z \cdot \kappa_s^d = 0, \forall s, d \in V \tag{4}$$

$$\aleph_{ij}^{sd} - Z \cdot \gamma_{ij_{idc}}^{sd} \leq 0, \forall i, j, s, d \in V \tag{5}$$

$$\aleph_{ij}^{sd} - \nabla_s^d \leq 0, \forall i, j, s, d \in V \tag{6}$$

$$-\aleph_{ij}^{sd} + \nabla_s^d + Z \cdot \gamma_{ij_{idc}}^{sd} \leq Z, \forall i, j, s, d \in V. \tag{7}$$

IP layer flow conservation constraints. Equation (8) formulates a flow conservation constraint (in the IP layer) at the source node for upstream DC and IDC demands. Thus, for an upstream data center demand, the source node is expected to utilize the desired bandwidth on the virtual links originating at the corresponding node whereas for an inter-data center demand, the source node is expected to utilize bandwidth on the virtual links without violating the amount of its workload that is not allowed to be migrated. Eq. (9) formulates the flow conservation constraint for the intermediate nodes while in Eq. (10), similar to Eq. (8), the flow conservation constraint for the destination nodes is formulated for the upstream DC and IDC demands

$$\begin{aligned} \left(D_{min}^s \cdot \Omega_s^{UP} + \ell_s \right) \leq &\sum_{d \in V} \sum_{j \in V} \Upsilon_{up}^{sd} \cdot \gamma_{sjup}^{sd} + \frac{\Upsilon_{IDC}^{sd} \cdot \aleph_{sj}^{sd}}{Z} \\ &- \sum_{d \in V} \sum_{j \in V} \Upsilon_{up}^{sd} \cdot \gamma_{jsup}^{sd} + \frac{\Upsilon_{IDC}^{sd} \cdot \aleph_{js}^{sd}}{Z} - \ell_s \cdot \kappa_s^s \\ &\leq \left(D_{max}^s \cdot \Omega_s^{UP} + \ell_s \right), \forall s \in V \end{aligned} \tag{8}$$

$$\begin{aligned} &\sum_{j \in V} \Upsilon_{up}^{sd} \cdot \gamma_{ijup}^{sd} + \frac{\Upsilon_{IDC}^{sd} \cdot \aleph_{ij}^{sd}}{Z} \\ &- \sum_{k \in V, k \neq j} \Upsilon_{up}^{sd} \cdot \gamma_{jkup}^{sd} + \frac{\Upsilon_{IDC}^{sd} \cdot \aleph_{jk}^{sd}}{Z} = 0, \forall i, s, d \in V \end{aligned} \tag{9}$$

$$\begin{aligned} -\left(D_{max}^s \cdot \Omega_s^{UP} + \ell_s \right) \leq &\sum_{d \in V} \sum_{j \in V} \Upsilon_{up}^{sd} \cdot \gamma_{djup}^{sd} \\ &+ \frac{\Upsilon_{IDC}^{sd} \cdot \aleph_{dj}^{sd}}{Z} - \sum_{d \in V} \sum_{j \in V} \Upsilon_{up}^{sd} \cdot \gamma_{jdup}^{sd} \\ &+ \frac{\Upsilon_{IDC}^{sd} \cdot \aleph_{jd}^{sd}}{Z} - \ell_s \cdot \kappa_s^s \\ &\leq -\left(D_{min}^s \cdot \Omega_s^{UP} + \ell_s \right), \forall s \in V. \end{aligned} \tag{10}$$

The constraints in Eqs. (11)-(12) ensure flow conservation in the IP layer for regular traffic between the core nodes and the downstream DC traffic. For detailed explanation of the constraints in Eqs. (11)-(12), the reader is referred to [10]

$$\begin{aligned} &\sum_{j \neq d, j \in V} \left(\Omega_{ds}^{DOWN} \cdot \gamma_{jd_{down}}^{ds} + \lambda_{jd}^{sd} \right) - \sum_{j \neq d, j \in V} \left(\Omega_{ds}^{DOWN} \cdot \gamma_{dj_{down}}^{ds} + \lambda_{dj}^{sd} \right) \\ &= \Lambda_{sd} + \Omega_{ds}^{DOWN}, \forall (s, d) \in V, s \neq d \end{aligned} \tag{11}$$

$$\sum_{j\neq s,d,j\in V}\left(\Upsilon^{ds}_{down}\cdot\gamma^{ds}_{ij_{down}}+\lambda^{sd}_{ij}\right)-\sum_{j\neq s,d,j\in V}\left(\Upsilon^{ds}_{down}\cdot\gamma^{ds}_{ji_{down}}+\lambda^{sd}_{ji}\right)$$
$$=0,\forall(s,d,i)\in V,d\neq i,s\neq i. \quad (12)$$

Capacity constraints. Equation (13) defines the capacity constraint ensuring that a virtual link has enough lightpath capacity to accommodate all types of demands traversing it

$$\sum_{s\in V}\sum_{d\in V}\Bigg(\lambda^{sd}_{ij}+\Upsilon^{sd}_{up}\cdot\gamma^{sd}_{ijup}+\Omega^{DOWN}_{ds}\cdot\gamma^{ds}_{ij_{down}} + \frac{\Upsilon^{sd}_{IDC}\cdot\aleph^{sd}_{ij}}{Z}\Bigg)-C\cdot C_{ij}\leq 0,\forall i,j\in V. \quad (13)$$

Manycast constraints for upstream DC and IDC demands. Equations (14)-(22) denote the constraints related to manycasting of upstream DC and IDC demands. Sufficient number of destinations is bounded below and above by D^s_{min} and D^s_{max} respectively. Reaching sufficient number of destinations by an upstream DC demand is ensured by Eqs. (14)-(15). Equation (16) ensures that an upstream DC demand can utilize at most one virtual link prior to reaching the destination node-d. In order to facilitate manycasting, the nodes must have multicast capability as formulated by Eq. (17). Thus, an upstream DC demand can be carried over the same virtual links up to node-j where the demand is split into multiple virtual links

$$\sum_{i\in V}\sum_{i\neq d}\Upsilon^{sd}_{up}\cdot\gamma^{sd}_{id_{up}}\leq D^s_{max}\cdot\Omega^{UP}_s,\forall s,d\in V \quad (14)$$

$$\sum_{i\in V}\sum_{i\neq d}\Upsilon^{sd}_{up}\cdot\gamma^{sd}_{id_{up}}\geq D^s_{min}\cdot\Omega^{UP}_s,\forall s,d\in V \quad (15)$$

$$\sum_{i\neq d,i\in V}\gamma^{sd}_{id_{up}}\leq 1,\forall s,d\in V \quad (16)$$

$$\sum_{d\in V}\gamma^{sd}_{ij_{up}}\leq 1,\forall s,i,j\in V. \quad (17)$$

By Eq. (18), it is guaranteed that at most one branch of the light-tree for the IDC demands can be connected to a possible destination node (i.e., data center). Eq. (19) formulates the workload conservation constraint denoting that the ratio of the workload migrated and the ratio of the workload hosted in a data center cannot exceed the initial workload of the corresponding data center. An IDC demand can utilize a link at most in one direction due to bidirectionality constraint as formulated in Eq. (20). The sum of the workload hosted in and migrated to a data center cannot exceed the maximum data center workload as shown in Eq. (21). Finally, as formulated by Eq. (22), the amount of the workload to be migrated from data center-s to data center-d takes its value based on either of the following three conditions: *i)* If s and d are the same data center, then, the ratio of the workload that will remain in the data center must be greater than or equal to a pre-specified minimum value, *ii)* It is zero if data center-d is not a potential workload receiver for data center-s, *iii)* Otherwise κ^d_s takes a value in $[0,1-\kappa_{MIN}]$

$$\sum_{i\in V}\aleph^{sd}_{id}\leq Z,\forall s,d\in V \quad (18)$$

$$\sum_{i\in V}\sum_{j\in V}\sum_{d\in V}\frac{\Upsilon^{sd}_{IDC}\cdot\aleph^{sd}_{ij}}{Z}+\ell_s\kappa^s_s=\ell_s,\forall s\in V \quad (19)$$

$$\aleph^{sd}_{ij}+\aleph^{sd}_{ji}\leq Z,\forall i,j,s,d\in V \quad (20)$$

$$\sum_{s\in V}\ell_s\cdot\kappa^d_s\leq\ell_{MAX},\forall d\in V \quad (21)$$

$$\kappa^d_s:\left\{\begin{array}{cc}\geq\kappa_{MIN} & s=d\\ =0 & \Upsilon^{sd}_{IDC}=0\\ \in[0,1-\kappa_{MIN}] & else\end{array}\right\},\ \forall s,d\in V. \quad (22)$$

Flow conservation constraint in the optical layer. Equations (23)-(24) denote the flow conservation constraints in the optical layer. Equation (23) ensures the following three conditions: *i)* the source node of a virtual link does not have any incoming wavelength channels, *ii)* The destination node of a virtual link does not have any outgoing wavelength channels. *iii)* A virtual link does not contain any loops. Equation (24) ensures that the number of lightpaths traversing a physical link-mn is limited by the total channel capacity of the fibers between node-m and node-n

$$W^{ij}_{mn}-W^{ij}_{nm}=\left\{\begin{array}{cc}-C_{ij} & m=i\\ C_{ij} & m=j\\ 0 & else\end{array}\right\},\ \forall m,n,i,j\in V \quad (23)$$

$$\sum_{i\in V}\sum_{j\in V}W^{ij}_{mn}-W\cdot f_{mn}\leq 0,\forall m,n\in V. \quad (24)$$

Cyber-physical constraints. In Eq. (25), the potential power consumption overhead of the upstream demand of node-s to data center-d is formulated by assuming that the potential increase in the workload of the data center, as well as the workload placement scheme running in the data center, is known in advance. $\Theta_{s,d}$ denotes the potential power consumption overhead that would be introduced to data center-d if the demands arriving at node-s are placed in data center-d. Hence, if any incoming link of node-d is utilized by the upstream demand initiated at node-s, power consumption overhead of the upstream data center demand of node-s to data center-d is $\Theta_{s,d}$, otherwise it is zero as the data center has not been selected out of the set of candidate destinations

$$\Phi^d_s=\sum_{j\neq d,j\in V}\Theta_{s,d}\cdot\gamma^{sd}_{jd_{up}}\forall s,d\in V. \quad (25)$$

3.2 SA-Based Heuristic for ToUP

In order to ensure polynomial time solution for the optimization model presented above, we propose a two-step heuristic which obtains an IDC traffic matrix in the first step, and in the second step reconfigures the inter-data center network to provision all types of demands in a ToU manner.

Step-1 - IDC workload migration. The first step is illustrated in Fig. 1 which is an SA-based approach. The notation used in the flowchart is as follows. Map is the main workload

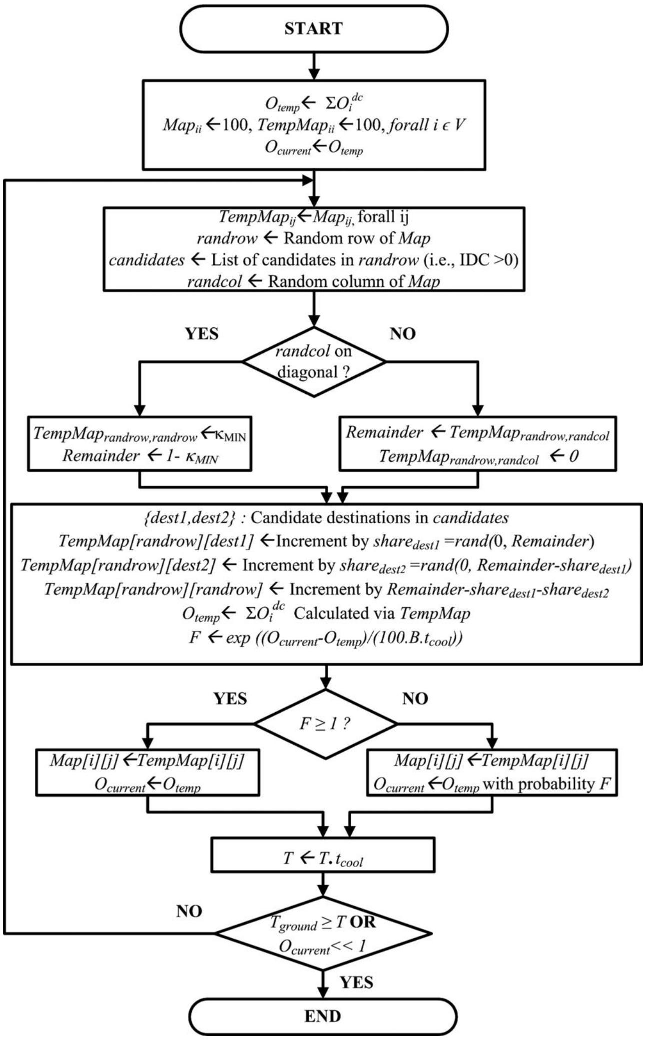

Fig. 1. Flowchart of inter-data center workload sharing.

distribution matrix whereas $TempMap$ denotes a temporary workload distribution matrix. O_{temp} and $O_{current}$ denote the initial Opex and current Opex, respectively whereas O_i^{dc} is the Opex of data center-i. T, B and t_{cool} are the simulated annealing-related settings denoting the annealing temperature, Boltzmann constant and cooling rate of the system, respectively. For IDC workload sharing, $\{dest1, dest2\}$ stands for the list of destination data centers, and its size is limited to two for the sake of simplicity, while κ_{MIN} represents the lower bound for the percentage of workload that has to be hosted in the current data center.

Initially, each cell of the diagonal of the workload migration matrix (Map) is 100 (i.e., $Map_{ii} = 100$) denoting that each data center initially keeps 100 percent of its workload within itself. The algorithm starts with an initial temperature and in each iteration, the system temperature cools down with the cooling rate, t_{cool}. At each iteration, the algorithm selects a row and a column randomly from the migration matrix, Map, and temporarily sets the selected cell at zero unless the corresponding cell is on the diagonal. If the selected cell is located on the diagonal, the algorithm temporarily sets its value to κ_{MIN}. Then, the altered value of the cell is distributed among DC_{MAX} cells and the corresponding cell. For the sake of simplicity, we illustrate the procedure for $DC_{MAX} = 2$ in the flowchart. Once the temporary distribution matrix, $TempMap$, is built, a new Opex value is calculated by using Eqs. (2)-(3). If this Opex value is less than the current Opex (i.e., $O_{temp} < O_{current}$ and $F \geq 1$), the new placement is accepted, and the initial Opex ($O_{current}$) is updated to be equal to the current temporary Opex (O_{temp}). Otherwise (i.e., $O_{temp} \geq O_{current}$ and $F \in [0, 1]$), a random number, r, is generated in the interval [0,1). If $r < F$, the new placement is accepted, and the current Opex is updated accordingly. Otherwise, if $r \geq F$, the solution is rejected. In the final step, the temperature is updated by the cooling rate, t_{cool}, (i.e., $T \leftarrow t_{cool} \times T$), and the algorithm goes back to the perturbation step to make a new move. SA converges if either of the following two conditions holds: *i*) For a temperature T, solutions do not improve for a reasonable number of iterations, and *ii*) Annealing temperature is equal to or less than the ground temperature ($T \leq T_{ground}$), i.e., the frozen state. Each iteration step has a runtime complexity of $O(N^2)$ due to the Opex calculation.

Step-2 - ToU-aware backbone virtualization. Once the IDC traffic mapping matrix is obtained, for every data center, its new load and corresponding processing and cooling power are used to assist provisioning the upstream DC and IDC demands. ToUP adopts the Delay and Power-Minimized Provisioning [10], as well as its routing and fiber and wavelength assignment (RFWA) functions. Therefore, while routing the IDC and upstream DC demands, ToUP ranks the candidate data centers based on the following two criteria: *i)* Minimum Opex, *ii)* Minimum path delay. ToUP selects $\lceil DC_{min}/2 \rceil$ of the destination data centers based on the minimum Opex ranking and $\lfloor DC_{min}/2 \rfloor$ of the destination data centers based on the minimum path length ranking where DC_{min} denotes the minimum number of data centers to be reached in order to provision the demand. Thus, similar to DePoMiP, ToUP also transforms the manycast demands into multiple unicast demands.

While routing a demand on the virtual topology, ToUP assigns link costs by running Eq. (26) where $Cost_{ij}^{v}(T)$ denotes the cost assigned to the virtual link-ij during the period T. In the equation link-ij denotes a virtual link which is formed by a set of physical links denoted by link-mn. According to the cost assignment function, ToUP aims at selecting the virtual links that are formed by lower physical cost ($Cost_{mn}^{phy}(T)$) and have available virtual link capacities. Cost assignment for the physical links is presented in Eq. (27). As seen in the equation, the physical link cost consists of the following three components: *i*) ToU prices at the corresponding location of node-n during the period T, *ii*) Power consumption of the network component along the link, *iii*) Length of the fiber-link. In the equation, W_{mn} denotes the remaining wavelength capacity in the physical link-mn. According to the physical cost assignment function, ToUP aims at selecting the links with shorter length, lower power consumption, and that are directed to the nodes experiencing lower ToU prices

$$Cost_{ij}^{v}(T) = \left\{ \begin{array}{cc} \sum\limits_{link-mn \in link-ij} Cost_{mn}^{phy}(T) & C'_{ij} > 0 \\ \infty & else \end{array} \right\} \quad (26)$$

TABLE 2
Regular Demands in the NSFNET throughout the Day (Gbps)

Hours / Nodes	01-03	04-06	07-09	10-12	13-15	16-18	19-21	22-24
9, 11, 12, 13, 14	40	40	40	90	90	110	80	100
7, 8, 10	50	30	30	70	90	100	100	100
4, 5, 6	100	40	30	30	90	90	110	80
1, 2, 3	80	30	30	50	100	90	110	80

$$Cost_{mn}^{phy}(T) = \left\{ \begin{array}{cc} \varphi_n(T) \cdot \Big[Lf_{mn} \cdot & \\ (P_e \cdot S_{mn} + P_t \cdot W_{mn}) \Big] & W_{mn} > 0 \\ \infty & else \end{array} \right\}. \quad (27)$$

ToUP ranks the data centers for IDC and upstream DC demands in $O(N^2)$ runtime complexity. The second step of the ToUP is the dominant part for the computational complexity of the algorithm since the RFWA is bounded above by $O(N^4)$.

4 Numerical Results

4.1 Simulation Settings

We evaluate the performance of ToUP in terms of overall Opex in the Cloud, Opex of the data center and network operators, power consumption and path delay of all demand types. As demand profiles are assumed to be forecasted, based on the forecasted demand profile, a static demand matrix is formed for each demand type. By running ToUP, the demands are provisioned under the newly reconfigured topology. Each data center is assumed to be associated with a network node and loaded at the beginning of the reconfiguration. An IP over WDM network is considered as the transmission medium under two topologies, namely the NSFNET [41] with 14 nodes and 21 links, and the European optical backbone network (EON) [42] which has 28 nodes and 41 links. Four different demand types are assumed as mentioned in Section 1.

In the IP-over-WDM network, each fiber link is assumed to consist of 16 wavelength channels, and each channel operates at 40 Gbps while EDFAs are placed at every 80 km. In the NSFNET topology, different time zones form four sets of nodes where the nodes in the same set experience the same demand profile. On the other hand, the demand profile in the EON topology is synthetically formed by using the demand profile in the NSFNET topology and considering the time differences between the zones. It is worthwhile mentioning that the demand profile varies significantly during the day and in medium term. Therefore, our aim is not to reflect the real demand profile in the corresponding regions but to investigate the performance of our proposal under various heterogeneous demand profile scenarios. Tables 2 and 3 show the demand profiles for the regular Internet demands during eight timeslots of the day in the NSFNET and EON topologies, respectively. In Table 3, WET, CET and EET nodes denote Western European Time, Central European Time and Eastern European Time zones, respectively. Upstream and downstream DC demands are

TABLE 3
Regular Demands in the EON throughout the Day (Gbps)

Hours / Nodes	01-03	04-06	07-09	10-12	13-15	16-18	19-21	22-24
WET nodes	30	30	90	90	110	80	100	40
CET nodes	30	90	90	110	80	100	40	30
EET nodes	90	90	110	80	100	40	30	30

assumed to be 0.2 and 1.5 times of the regular demands, respectively [31]. The IDC demand profiles are determined by ToUP. In each timeslot, the Cloud backbone switches to a new virtual topology to meet the objective and the constraints of the corresponding provisioning scheme.

In the transport network, an EDFA and a transponder are assumed to consume 8 and 73 W, respectively, whereas an IP router port consumes 1,000 W [39]. For the NSFNET topology, we have obtained the monthly electricity price of each location from the US Energy Information Administration [43] assuming that these prices denote the mid-peak ToU prices. For the EON topology, we have used Europe's energy portal to obtain average price for electricity consumption (in terms of EUR/kWh) [44]. Then we have obtained the ToU rates through the numerical values provided by Hydro Ottawa [45]. In [45], off-peak hours during the winter period denote 7:00pm-06:59am, and subscribers are charged by $P'^{OFFPEAK}$ whereas mid-peak hours correspond to 11:00 am-4:59 pm, and customers are charged by P'^{MID}. The remaining hours of the day (i.e., 7:00 am-10:59 am, 5:00 pm-6:59 pm) form the peak times where the customers are charged by P'^{PEAK}. We have adopted the formulation in [19] to obtain the peak and off-peak ToU prices for each node location-i as shown in Eqs. (28)-(29). Figs. 2 and 3 illustrate the ToU prices obtained for each node location in the NSFNET and EON topologies, respectively. It is worthwhile mentioning that, in all plots, we use Eastern Standard Time (EST) as a reference for the x-axes

$$P_i^{PEAK} = P_i^{MID} + \frac{(P'^{PEAK} - P'^{MID})}{P'^{MID}} \cdot P_i^{MID} \quad (28)$$

$$P_i^{OFFPEAK} = P_i^{MID} - \frac{(P'^{MID} - P'^{OFFPEAK})}{P'^{MID}} \cdot P_i^{MID}. \quad (29)$$

It is assumed that Minimizing Heat Recirculation (MHR) [46] runs for workload placement in a data center while a

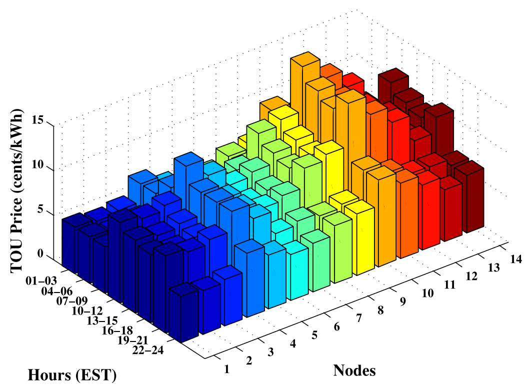

Fig. 2. Time of Use prices for each node in the NSFNET.

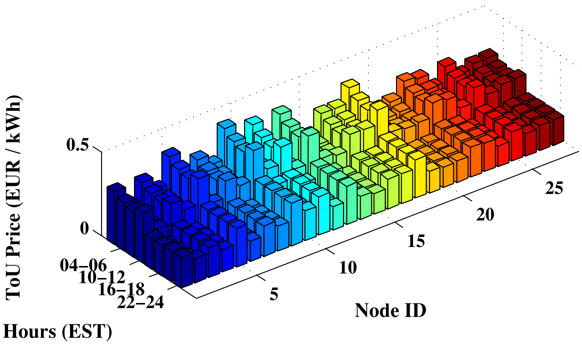

Fig. 3. ToU prices in the European backbone throughout the day.

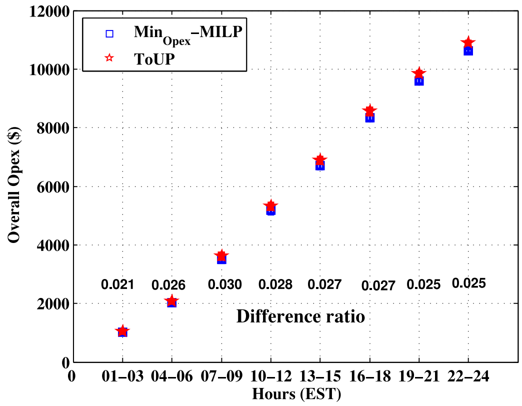

Fig. 4. Cumulative Opex comparison under ToUP and the MILP formulation.

data center is assumed to consume 168 kW (100 kW) of idle IT (cooling) power and 319.2 kW (280 kW) of full utilization IT (cooling) power. A data center is assumed to have an initial load between 0.1 and 0.8 whereas an incoming workload submission/migration is assumed to increase the data center workload between 0.025 and 0.2. For each demand of the IDC traffic and upstream DC traffic, the number of candidate destinations is either 3 or 4 while the desired number of destinations is fixed to 2. Either 2, 3 or 4 data centers are assumed to originate a downstream DC demand which is aggregated at the destination backbone node. It is worthwhile noting that only the IDC demands and the upstream DC demands are provisioned based on manycast whereas the rest of the demand types are provisioned based on unicast routing. Today, a cloud data center hosts thousands of servers which can be estimated to drain over some hundred mega-watts of power from the grid. For instance in 2009, more than 300,000 servers were estimated to be hosted in Microsoft's Chicago data center [47]. However, the aim of this study is showing the advantages of our proposal under a small scale data center scenario. Therefore the scope of the simulations is limited to a small scale experimental scenario in [46]. The proposal can be adapted to a large-scale Cloud data center scenario in later stages.

In the first step of the ToUP heuristic, the Boltzmann constant is set to 0.01 while the cooling rate is considered to be 0.95. The termination parameters, i.e., ground temperature and the minimum temperature change, are taken as 0.005 and 0.001, respectively.

4.2 MILP-Based Model vs. ToUP

In this section, we verify ToUP by comparing the heuristic results to the results obtained under the MILP. Hereafter, we use ToUP to denote the two-step ToUP heuristic. To this end, we test the ToUP under a simple scenario where NSFNET topology is considered as the transport medium. In these test scenarios, in order to obtain results in feasible time, we set $\kappa_{MIN} = 1$ in the MILP and the ToUP heuristic so that the IDC constraints are eliminated.

Fig. 4 compares ToUP and the solution of the MILP in terms of overall Opex in the inter-data center network. As seen in the figure, ToUP introduces higher Opex when compared to the MILP formulation however, this difference is at the order of 3 percent. Fig. 5 illustrates the comparison of ToUP and the MILP-based solutions in terms of power consumption in the inter-data center network, and the additional power consumption of ToUP is at most 1.7 percent of the power consumption obtained by the solution of the MILP formulation.

In Fig. 6, ToUP is compared to the MILP solution in terms of average path delay of any demand type. Similar to the previous comparisons, average additional path delay introduced by ToUP is within a few per cent of the path delay introduced by the MILP solution, and it is less than a half millisecond.

Indeed, ToUP is designed to provide a sub-optimal solution for this problem. Therefore, deviation from the solution of MILP-based model should be expected. However, based on the deviation from the MILP-based solution in the simulation results, it can be concluded that ToUP can be adapted to a real-time large-scale scenario where solving an MILP-based model may lead to significantly long run times.

4.3 Performance Evaluation of ToUP

As ToUP has been verified under a small-scale scenario in the previous section, in this section, we evaluate the performance of ToUP under various test cases. Previous work reports that Delay-Minimized Provisioning (DeMiP) consumes the highest amount of power in the network whereas Delay and Power Minimized Provisioning consumes the least power [10]. Therefore, in the Opex and power saving plots, we use DeMiP as the benchmark solution to the inter-data center network design, and evaluate ToUP and the energy efficient provisioning models in the context of ToU with respect to their savings over DeMiP. Here, we assume

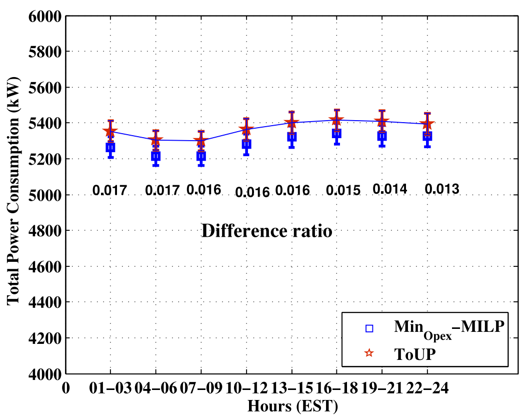

Fig. 5. Power consumption comparison under ToUP and the MILP formulation.

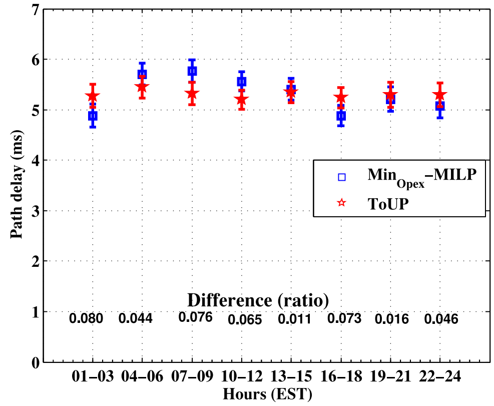

Fig. 6. Average path delay comparison under ToUP and the MILP formulation.

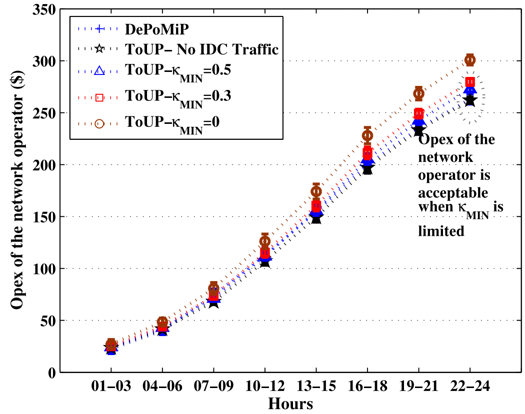

Fig. 8. Cumulative Opex of the network operator under DePoMiP, ToUP and ToUP with no IDC traffic under the NSFNET topology.

that the calculated power is constantly consumed by the network and/or data center operators so that we are able to calculate the electricity cost at the end of each timeslot.

4.3.1 Results under the NSFNET Topology

In Fig. 7, we compare the electricity cost of the inter-data center network under ToUP to that under DePoMiP. Since we also aim at investigating the impact of κ_{MIN} on the performance of the inter-data center network, we vary κ_{MIN} between 0 and 1. Fig. 7 shows that the lower the κ_{MIN}, the higher the Opex savings with respect to DeMiP. Moreover, the electricity cost under ToUP without IDC workload sharing is closer to that under DeMiP. Running ToUP with unlimited IDC traffic allowance (i.e., $\kappa_{MIN} = 0$) enables workloads to be migrated to the data centers where lower ToU rates are experienced. On the other hand, unlimited workload migration among data centers may introduce a drawback to the network operator as shown in Fig. 8. In the figure, cumulative Opex of the network operator under ToUP without IDC traffic, ToUP with $\kappa_{MIN} \geq 0.3$ and DePoMiP outperform ToUP with unlimited migration between data centers. Considering the results in Figs. 7 and 8, ToUP with $\kappa_{MIN} = 0.3$ has a similar behavior to the unlimited workload migration in terms of Cloud Opex savings while its behavior in terms of network operator's Opex is similar to ToUP without IDC traffic.

Fig. 9 illustrates the power savings of ToUP without IDC traffic, ToUP and DePoMiP with respect to DeMiP. Since the data centers are the most power hungry part of a Cloud network, ToUP outperforms the power saving performance of DePoMiP if IDC traffic is allowed. Furthermore lower κ_{MIN} values lead to more savings in power consumption. ToUP enables re-distributing the data center workloads so that the data centers that experience the lowest ToU rates tend to receive the majority of the demands that are already placed in the Cloud. Therefore, the lower the ratio of the workload to be kept in its original host, the higher the probability of finding an alternate host which will introduce lower Opex.

In Fig. 10a, we present the upstream DC delays for DeMiP, DePoMiP and ToUP. The overhead of ToUP in terms of path delay is less than 1 ms when compared to DeMiP. Moreover, ToUP adopts the virtual and physical link cost assignment functions of DePoMiP and extends them by including ToU rates to minimize Opex for the Cloud. Including ToU-awareness increases the chance to select closer data centers when they are experiencing lower ToU rates. Therefore, regardless of the value of κ_{MIN}, ToUP can introduce lower path delays when compared to DePoMiP.

In Fig. 10b, we present the impact of κ_{MIN} on the path delay of the IDC traffic. $\kappa_{MIN} = 1$ denotes no IDC traffic; hence in order to investigate the effect of allowing less intense migration among the data centers, we have tested

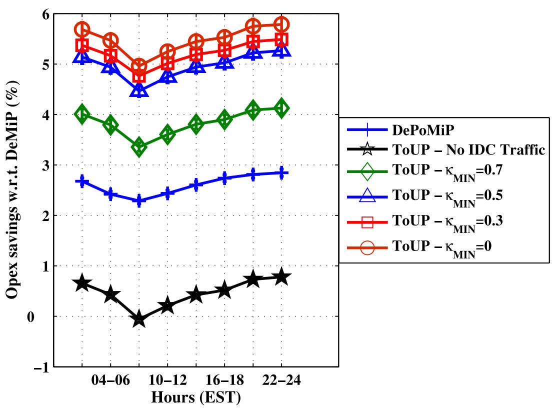

Fig. 7. Total savings in the electricity bill by DePoMiP, ToUP and ToUP with no IDC traffic under the NSFNET topology.

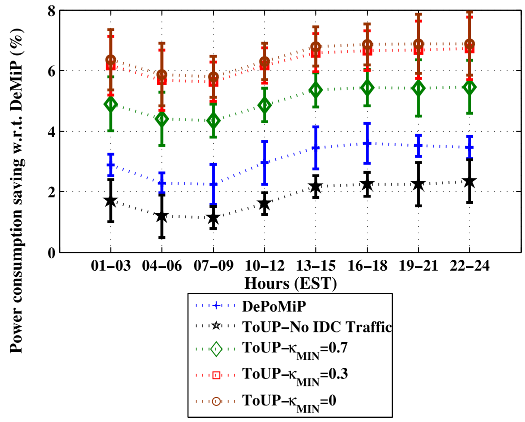

Fig. 9. Savings in total power consumption under DePoMiP, ToUP and ToUP with no IDC traffic under the NSFNET topology across all operators.

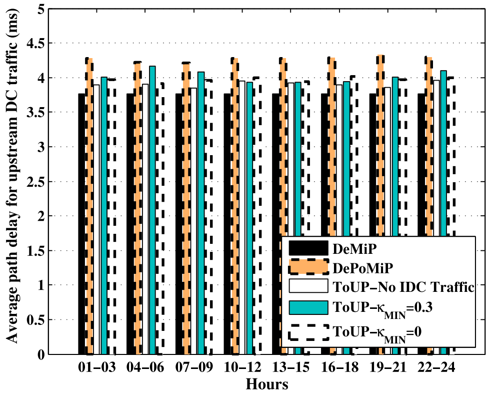

(a)

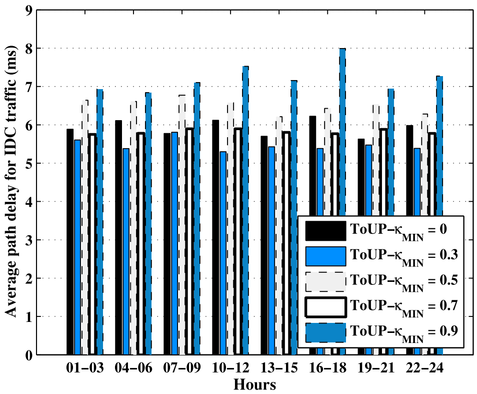

(b)

Fig. 10. Path delay performance (a) Upstream data center traffic, (b) IDC traffic under ToUP.

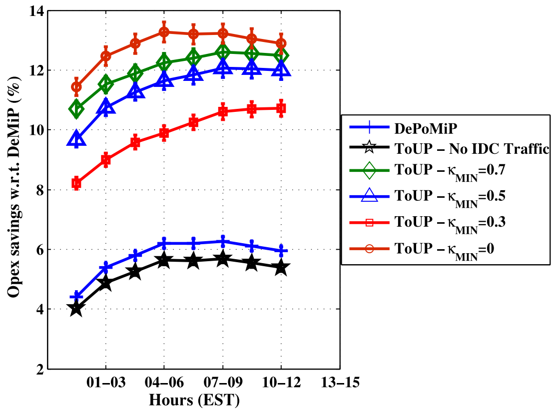

Fig. 11. Total savings in the electricity bill in the EON under DePoMiP, ToUP and ToUP with no IDC traffic under the EON.

ToUP with also $\kappa_{MIN} = 0.9$. In all cases, $\kappa_{MIN} = 0.3$ and $\kappa_{MIN} = 0.7$ introduce the lowest IDC path delays. In case of $\kappa_{MIN} = 0.5$, any data center is allowed to migrate half of its workload increasing the network traffic. Unlike the situation under $\kappa_{MIN} = 0.3$, ToUP will be forced to utilize the existing virtual links rather than adding new virtual links and routing them via shorter paths. Hence, IDC delay results further confirm that selection of an appropriate upper limit for the ratio of the workload allowed to be migrated to other data centers introduces the advantage of ToU-awareness in an inter-data center network virtualization in terms of path delay, as well as Opex and energy/power consumption.

4.3.2 Results under the EON Topology

We further investigate the effect of topological properties on the performance of ToUP. In Fig. 11, unlike the performance under the NSFNET, ToUP without IDC traffic can still save power that is close to the savings of DePoMiP. Furthermore it is more beneficial to set κ_{MIN} at greater values ($\kappa_{MIN} \geq 0.5$) under the EON topology when compared to the test cases under the NSFNET topology to ensure high Opex savings. It is worthwhile mentioning that $\kappa_{MIN} = 0.3$ can still lead to significant savings when compared to ToUP without IDC traffic and DePoMiP. This is due to the high connectivity of the EON topology, as well as the diversity of electricity prices due to the large number of nodes associated with diverse authorities. On the other hand, allowing a data center to migrate its entire workload leads to higher power savings as data centers are the dominating factor for power consumption in the Cloud network. As seen in Fig. 12, when the ToU prices are low and close to each other (e.g., between 16:00 and 00:59 EST), limiting the workload migration ratio ($\kappa_{MIN} \geq 0.3$) shows similar behavior to ToUP with unlimited workload migration among data centers. The reason of this behavior is that there is not a significant difference in ToU prices during this period. Furthermore the corresponding period (e.g., between 16:00 and 00:59 EST) does not contain the timeslots when all regions experience on-peak pricing. For the sake of clarity, we do not present the results for the other κ_{MIN} values in the figure.

Despite the overall Opex which is mostly dominated by the expenses of the data center operator, it is worth studying the Opex of the network operator, as well. Fig. 13 illustrates the cumulative Opex performance of the network operator. The results are similar to those collected under the NSFNET topology. Thus, keeping the workload within the initial host introduces significant Opex savings to the network operator. However, selecting appropriate workload migration ratios, i.e., setting κ_{MIN} to an appropriate value, can address the trade-off between the Opex of the network and data center operators.

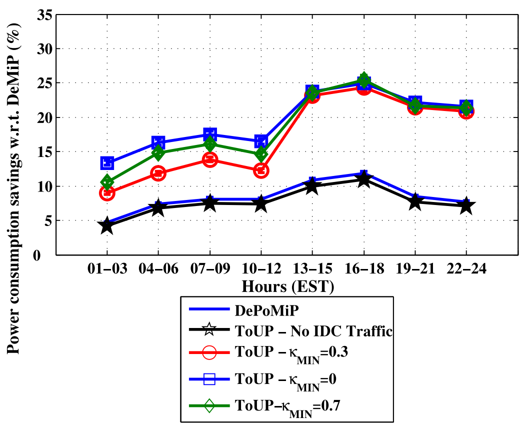

Fig. 12. Total power savings in the EON under DePoMiP, ToUP and ToUP with no IDC traffic.

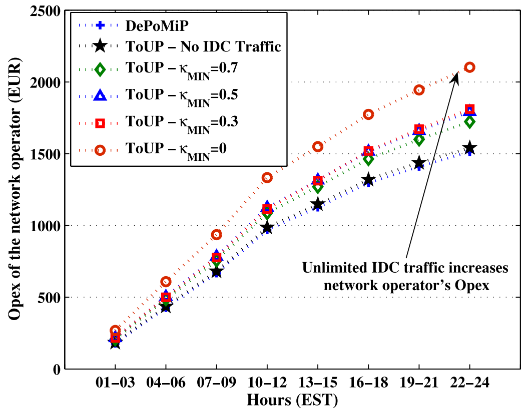

Fig. 13. Cumulative Opex of the network operator in the EON under DePoMiP, ToUP and ToUP with no IDC traffic.

We have further evaluated the path delay performance of ToUP under EON, and obtained similar results to those under Figs. 10a and 10b. Moreover we have also investigated the path delay for upstream DC, downstream DC and regular demands. Under both topologies, we have seen that ToUP does not increase the path delays of these demand types.

5 Conclusion and Future Work

In this paper, we have studied the ToU-aware design of a virtual inter-data center network in order to minimize the electricity bills of the operators and reduce the energy consumption throughout the Cloud. To this end, we have proposed ToU-aware provisioning where data centers and the inter-data center network interact with the smart grid network in order to minimize the electricity bills of the operators. According to the proposed framework, each data center is allowed to migrate a certain amount of its workload to a certain number of destination data centers. Along with an MILP formulation, we have proposed a two-step heuristic solution in order to reconfigure the virtual inter-data center network based on the forecasted demand profiles when needed. The first step of the heuristic runs a simulated annealing-based algorithm to determine the workload migration among the data centers, which is followed by provisioning various types of demands via a ToU-aware virtual topology mapping function. We have verified the efficiency of ToUP by comparing it to the MILP-based solution under a small scale scenario, and evaluated the performance of ToUP under various medium-scale scenarios. We have shown that when the amount of workload to be migrated is bounded above at each data center, electricity bills of both cloud and network operators can be reduced significantly when compared to a previously proposed approach which only aims at minimum energy consumption. Moreover, we have shown that ToUP leads to further power consumption savings in the Cloud when each data center is enforced to keep a certain amount of its original workload.

Future extensions of this study include a holistic design scheme which considers virtual machine placement and migration constraints in the data centers, as well as Service Level Agreement (SLA) guarantees.

Acknowledgments

B. Kantarci was with the School of Electrical Engineering and Computer Science at the University of Ottawa.

References

[1] H. T. Mouftah and B. Kantarci, *Communication Infrastructures for Cloud Computing*. Hershey, PA, USA: IGI Global, 2013.
[2] Q. Zhang, L. Cheng, and R. Boutaba, "Cloud computing: State-of-the-art and research challenges," *J. Internet Serv. Appl.*, vol. 1, pp. 7–18, May 2010.
[3] J-W. Lin, C-H. Chen, and J. M. Chang, "QoS-aware data replication for data-intensive applications in cloud computing systems," *IEEE Trans. Cloud Comput.*, vol. 1, no. 1, pp. 101–115, Jan.–Jun. 2013.
[4] L. Parolini, B. Sinopoli, B. H. Krogh, and Z. Wang, "A cyber-physical systems approach to data center modeling and control for energy efficiency," *Proc. IEEE*, vol. 100, no. 1, pp. 254–268, Jan. 2012.
[5] Y. Guo, Z. Ding, Y. Fang, and D. Wu, "Cutting down electricity cost in internet data centers by using energy storage," in *Proc. IEEE Global Telecommun. Conf.*, Dec. 2011, pp. 1–5.
[6] J. Baliga, R. W. A. Ayre, K. Hinton, and R. S. Tucker, "Green cloud computing: Balancing energy in processing, storage, and transport," *Proc. IEEE*, vol. 99, no. 1, pp. 149–167, Jan. 2011.
[7] A. Beloglazov, J. Abawajy, and R. Buyya, "Energy-aware resource allocation heuristics for efficient management of data centers for cloud computing," *Future Generation Comput. Syst.*, vol. 28, no. 5, pp. 755–768, 2012.
[8] A. Corradi, M. Fanelli, and L. Foschini, "VM consolidation: A real case based on OpenStack cloud," *Elsevier Future Generation Comput. Syst.*, vol. 32, pp. 118–127, 2012.
[9] H. Viswanathan, E. K. Lee, and D. Pompili, "Self-organizing sensing infrastructure for autonomic management of green datacenters," *IEEE Netw.*, vol. 25, no. 4, pp. 34–40, Jul./Aug. 2011.
[10] B. Kantarci and H. T. Mouftah, "Designing an energy-efficient cloud network," *IEEE/OSA J. Opt. Commun. Netw.*, vol. 4, no. 11, pp. B101–B113, Nov. 2012.
[11] C. Develder, M. De Leenheer, B. Dhoedt, M. Pickavet, D. Colle, F. De Turck, and P. Demeester, "Optical networks for grid and cloud computing applications," *Proc. IEEE*, vol. 100, no. 5, pp. 1149–1167, May 2012.
[12] B. Kantarci, L. Foschini, A. Corradi, and H. T. Mouftah, "Design of energy-efficient cloud systems via network and resource virtualization," *Int. J. Netw. Manage.*, doi: 201310.1002/nem.1838, Aug. 2013.
[13] M. F. Bari, R. Boutaba, R. Esteve, L. Z. Granville, M. Podlensy, M. G. Rabbani, and Q. Zhang, "Data center network virtualization: A survey," *IEEE Commun. Surveys Tuts.*, vol. 5, no. 2, pp. 909–928, Second Quarter 2013.
[14] G. Sun, V. Anand, D. Liao, C. Lu, X Zhang, and N-H. Bao, "Power-efficient provisioning for online virtual network requests in cloud-based data centers," *IEEE Syst. J.*, 2014, doi: 10.1109/JSYST.2013.2289584.
[15] E. Celebi and J. D. Fuller, "Time-of-use pricing in electricity markets under different market structures," *IEEE Trans. Power Syst.*, vol. 27, no. 3, pp. 1170–1181, Aug. 2012.
[16] L. P. Qian, Y. J. Zhang, J. Huang, and Y. Wu, "Demand response management via real-time electricity price control in smart grids," *IEEE J. Sel. Areas Commun.*, vol. 31, no. 7, pp. 1268–1280, Jul. 2013.
[17] T. Hahn, Z. Tan, and W. Ko, "Design of time-varying rate considering CO_2 emission," *IEEE Trans. Smart Grid*, vol. 4, no. 1, pp. 383–389, Mar. 2013.
[18] R. de Sa Ferreira, L. A. Barroso, P. R. Lino, M. M. Carvalho, and P. Valenzuela, "Time-of-use tariff design under uncertainty in price-elasticities of electricity demand: A stochastic optimization approach," *IEEE Trans. Smart Grid*, vol. 4, no. 4, pp. 2285–2295, Dec. 2013.
[19] B. Kantarci and H. T. Mouftah, "The impact of time of use (tou)-awareness in energy and opex performance of a cloud backbone," in *Proc. IEEE Global Telecommun. Conf.*, Dec. 2012, pp. 3250–3255.
[20] B. Kantarci and H. T. Mouftah, "Time of use (ToU)-awareness with inter-data center workload sharing in the cloud backbone," in *Proc. IEEE Int. Conf. Commun.*, Jun. 2013, pp. 4207–4211.
[21] Q. Zhang, Q. Zhu, and R. Boutaba, "Dynamic resource allocation for spot markets in cloud computing environments," in *Proc. IEEE/ACM Int. Conf. Utility Cloud Comput.*, Dec. 2011, pp. 178–185.

[22] E. Caron, F. Desprez, and A. Muresan, "Forecasting for grid and cloud computing on-demand resources based on pattern matching," in *Proc. IEEE Int. Conf. Cloud Comput. Technol. Sci.*, Dec. 2010, pp. 456–463.

[23] J. J. Prevost, K. Nagothu, B. Kelley, and M. Jamshidi, "Prediction of cloud data center networks loads using stochastic and neural models," in *Proc. Int. Conf. Syst. Syst. Eng.*, Jun. 2011, pp. 276–281.

[24] Z. Zhang, H. Wang, L. Xiao, and L. Ruan, "A statistical based resource allocation scheme in cloud," in *Proc. Int. Conf. Cloud Services Comput.*, Dec. 2011, pp. 266–273.

[25] C. Cavdar, A. Yayimli, and L. Wosinska, "How to cut the electric bill in optical WDM networks with time-zones and time-of-use prices," in *Proc. 37th Eur. Conf. Expo. Opt. Commun.*, Sep. 2011, p. We.10.P1.92.

[26] M. S. Ilyas, S. Raza, C-C. Chen, Z. A. Uzmi, and C.-N. Chuah, "RED-BL: Energy solution for loading data centers," in *Proc. IEEE Conf. Comput. Commun.*, Mar. 2012, pp. 2866–2870.

[27] Y. Zhang, Y. Wang, and X. Wang, "Electricity bill capping for cloud-scale data centers that impact the power markets," in *Proc. Int. Conf. Parallel Process.*, Sep. 2012, pp. 440–449.

[28] H. T. Mouftah and B. Kantarci, "Energy-efficient cloud computing: A green migration of the traditional IT," in *Handbook on Green Communication and Systems*, M. S. Obaidat, A. Anpalagan, and I. Woungang, Eds. Amsterdam, The Netherlands: Elsevier, 2012, pp. 295–330.

[29] J. Buysse, C. Cavdar, M. de Leenheer, B. Dhoedt, and C. Develder, "Improving energy efficiency in optical cloud networks by exploiting anycast routing," in *Proc. SPIE Conf. Ser.*, Nov. 2011, pp. 1–6.

[30] D. Tafani, B. Kantarci, H. T. Mouftah, C. McArdle, and L. P. Barry, "Distributed management of energy-efficient lightpaths for computational grids," in *Proc. IEEE Global Telecommun. Conf.*, Dec. 2012, pp. 2924–2929.

[31] X. Dong, T. El-Gorashi, and J. M. H. Elmirghani, "Green IP over WDM networks with data centers," *IEEE/OSA J. Lightw. Technol.*, vol. 29, no. 12, pp. 1861–1880, Jun. 2011.

[32] X. Dong, T. El-Gorashi, and J. M. H. Elmirghani, "Use of renewable energy in an IP over WDM network with data centres," *IET Optoelectron.*, vol. 6, no. 4, pp. 155–164, Aug. 2012.

[33] M. Gattulli, M. Tornatore, R. Fiandra, and A. Pattavina, "Low-carbon routing algorithms for cloud computing services in IP-over-WDM networks," in *Proc. Int. Conf. Commun.*, Jun. 2012, pp. 3032–3036.

[34] J. Doyle, R. Shorten, and D. O'Mahony, "Stratus: Load balancing the cloud for carbon emissions control," *IEEE Trans. Cloud Comput.*, vol. 1, no. 1, pp. 116–128, Jan.–Jun. 2013.

[35] F. Larumbe and B. Sanso, "A tabu search algorithm for the location of data centers and software components in green cloud computing networks," *IEEE Trans. Cloud Comput.*, vol. 1, no. 1, pp. 22–35, Jan.–Jun. 2013.

[36] A. Amokrane, M. F. Zhani, R. Langar, R. Boutaba, and G. Pujolle, "Greenhead: Virtual data center embedding across distributed infrastructures," *IEEE Trans. Cloud Comput.*, vol. 1, no. 1, pp. 36–49, Jan.–Jun. 2013.

[37] X. Lu, W. Wang, and J. Ma, "An empirical study of communication infrastructures towards the smart grid: Design, implementation, and evaluation," *IEEE Trans. Smart Grid*, vol. 4, no. 1, pp. 170–183, Mar. 2013.

[38] M. Jinno, and Y. Tsukishima, "Virtualized optical network (VON) for agile cloud computing environment," in *Proc. Opt. Fiber Commun. Conf.*, Mar. 2009, pp. 1–3.

[39] G. Shen and R. S. Tucker, "Energy-minimized design for IP over WDM networks," *IEEE/OSA J. Opt. Commun. Netw.*, vol. 1, no. 1, pp. 176–186, Jun. 2009.

[40] R. Prasad and H. Wu, "Gateway deployment optimization in cellular Wi-Fi mesh networks," *J. Netw.*, vol. 1, no. 3, pp. 31–38, Jul. 2006.

[41] B. Kantarci and H. T. Mouftah, "Energy-efficient cloud services over wavelength-routed optical transport networks," in *Proc. IEEE Global Telecommun. Conf.*, Dec. 2011, pp. SAC06.6.1–SAC06.6.5.

[42] S. Maesschalck, D. Colle, I. Lievens, M. Pickavet, P. Demeester, and C. Mauz, "Pan-european optical transport networks: An availability-based comparison," *Photon. Netw. Commun.*, vol. 5, pp. 203–225, 2003.

[43] (2012, Mar.). U.S. Energy Information Administration [Online]. Available: http://www.eia.gov

[44] (2012, Aug.). Europe's Energy Portal [Online]. Available: http://www.energy.eu

[45] (2012, Mar.). Hydro Ottawa [Online] http://www.hydroottawa.com

[46] J. Moore, J. Chase, P. Ranganathan, and R. Sharma, "Making scheduling cool: Temperature-aware workload placement in data centers," in *Proc. USENIX Annu. Tech. Conf.*, Apr. 2005, pp. 61–74.

[47] R. Miller. (2009, May). Who Has the Most Web Servers? Data Center Knowledge [Online]. Available: http://www.datacenterknowledge.com/archives/2009/05/14/whos-got-the-most-web-servers/

Burak Kantarci (S'05, M'09, SM'12) received the MSc and PhD degrees in computer engineering from Istanbul Technical University in 2005, and 2009, respectively. He is an assistant professor in the Department of Electrical and Computer Engineering at Clarkson University. Prior to joining Clarkson, he was a postdoctoral fellow at the School of Electrical Engineering and Computer Science of the University of Ottawa. He received the Siemens Excellence Award in 2005 for his studies in optical burst switching. During his PhD study, he studied as a visiting scholar at University of Ottawa where he completed the major content of his thesis. He has coauthored more than seven-dozen papers in established journals and conferences, and contributed to nine book chapters. He is the coeditor of the book entitled *Communication Infrastructures for Cloud Computing*. He serves in the editorial board of *IEEE Communications Surveys and Tutorials*. He also serves as an information officer for the IEEE Technical Committee on Sustainable Computing(June 2014-present). His research interests are energy-efficient network planning, cloud computing, green communications, and mobile networks. He is a senior member of the IEEE.

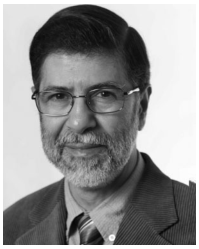

Hussein T. Mouftah (S'74, M'76, SM'80, F'90) joined the School of Electrical Engineering and Computer Science of the University of Ottawa in 2002 as a Tier 1 Canada Research chair professor, where he became a University distinguished professor in 2006. He has been with the ECE Department at Queen's University (1979-2002), where he was prior to his departure a full professor and the department associate head. He has six years of industrial experience mainly at Bell Northern Research of Ottawa (now Nortel Networks). He served as an editor-in-chief of the *IEEE Communications Magazine* (1995-97) and *IEEE ComSoc Director of Magazines* (1998-99), chair of the Awards Committee (2002-03), director of Education (2006-07), member of the Board of Governors (1997-99 and 2006-07), and member of the Nomination Committee (since 2012-). He has been a distinguished speaker of the IEEE Communications Society (2000-2007). He is the author or coauthor of nine books, 63 book chapters and more than 1300 technical papers, 12 patents and 142 industrial reports. He is the joint holder of 18 Best Paper and/or Outstanding Paper Awards. He has received numerous prestigious awards, such as the 2007 Royal Society of Canada Thomas W. Eadie Medal, the 2007-2008 University of Ottawa Award for Excellence in Research, the 2008 ORION Leadership Award of Merit, the 2006 IEEE Canada McNaughton Gold Medal, the 2006 EIC Julian Smith Medal, the 2014 EIC Y. K. Lo Medal, the 2004 IEEE ComSoc Edwin Howard Armstrong Achievement Award, the 2004 George S. Glinski Award for Excellence in Research of the U of O Faculty of Engineering, the 1989 Engineering Medal for Research and Development of the Association of Professional Engineers of Ontario (PEO), and the Ontario Distinguished Researcher Award of the Ontario Innovation Trust. He is a fellow of the IEEE (1990), the Canadian Academy of Engineering (2003), the Engineering Institute of Canada (2005) and the Royal Society of Canada RSC Academy of Science (2008).